articles

molecular pharmaceutics

Celecoxib:Nicotinamide Dissociation: Using Excipients To Capture the Cocrystal's Potential

Julius F. Remenar,*,† Matthew L. Peterson,† Peter W. Stephens,‡ Zhong Zhang,† Yuri Zimenkov,† and Magali B. Hickey†

TransForm Pharmaceuticals, Inc., 29 Hartwell Avenue, Lexington, Massachusetts 02421, and Department of Physics & Astronomy, Stony Brook University, Stony Brook, New York 11794-3800

Received January 15, 2007; Revised Manuscript Received April 27, 2007; Accepted April 30, 2007

Abstract: The cocrystal of celecoxib and nicotinamide (**Cel:Nic**) was crystallized from chloroform in a 1:1 ratio, and the structure has been solved from powder X-ray diffraction data. The dissolution and solubility of **Cel:Nic** are medium dependent and can be attributed to differences in conversion of **Cel:Nic** to celecoxib polymorphs I and III (**Cel-I** and **Cel-III**). The presence of low concentrations of surfactants facilitates the rapid conversion of neat **Cel:Nic** to large aggregates of **Cel-III** that dissolve more slowly than commercial **Cel-III** into 1% SDS solution. In contrast, combinations of **Cel:Nic** with both 1−10% solid SDS and PVP wet rapidly and convert to a mixture of amorphous celecoxib and a micron-sized crystalline celecoxib form IV (**Cel-IV**), which has recently been shown to be up to 4-fold more bioavailable than marketed **Cel-III**. More than 90% of the suspended material dissolves within 2 min at 37 °C when transferred to 1% SDS solution. This example highlights the importance of exploring the form conversion of cocrystals in aqueous media prior to pharmacokinetic studies, and illustrates the potential of simple formulations to overcome the limitations caused by rapid dissociation of cocrystals and recrystallization of poorly soluble forms in aqueous media.

Keywords: Polymorphs; pharmaceutical; cocrystal; nicotinamide; morphology; dissolution; stability; celecoxib; formulation

Introduction

The study of pharmaceutical cocrystals has been expanding rapidly since 2003 as evidenced by the growing number of publications and patent applications over the past four years.[1−12] The literature has focused primarily on structure and dissolution properties of cocrystals and on techniques for preparing them.[3,4,8−11,13] Prior to 2003, only a few examples involving the use of pharmaceutical cocrystals were reported.[14−18] Recently, separate studies by McNamara and Variankaval have shown substantial increases in bioavail-

* To whom correspondence should be addressed. Mailing address: TransForm Pharmaceuticals, Inc., 29 Hartwell Avenue, Lexington, MA 02421. E-mail: JRemenar@tpius.jnj.com. Tel: 781-674-8000. Fax: 781-863-6519.

† TransForm Pharmaceuticals, Inc.

‡ Stony Brook University.

(1) Almarsson, O.; Zaworotko, M. J. Crystal engineering of the composition of pharmaceutical phases. Do pharmaceutical cocrystals represent a new path to improved medicines? *Chem. Commun.* **2004**, *17*, 1889−1896.

(2) Childs, S. L.; Chyall, L. J.; Dunlap, J. T.; Smolenskaya, V. N.; Stahly, B. C.; Stahly, G. P. Crystal Engineering Approach To Forming Cocrystals of Amine Hydrochlorides with Organic Acids. Molecular Complexes of Fluoxetine Hydrochloride with Benzoic, Succinic, and Fumaric Acids. *J. Am. Chem. Soc.* **2004**, *126* (41), 13335−13342.

(3) Fleischman, S. G.; Kuduva, S. S.; McMahon, J. A.; Moulton, B.; Bailey Walsh, R. D.; Rodriguez-Hornedo, N.; Zaworotko, M. J. Crystal Engineering of the Composition of Pharmaceutical Phases: Multiple-Component Crystalline Solids Involving Carbamazepine. *Cryst. Growth Des.* **2003**, *3* (6), 909−919.

(4) Jayasankar, A.; Somwangthanaroj, A.; Shao, Z. J.; Rodriguez-Hornedo, N. Cocrystal Formation during Cogrinding and Storage is Mediated by Amorphous Phase. *Pharm. Res.* **2006**, *23* (10), 2381−2392.

10.1021/mp0700108 CCC: $37.00
Published on Web 05/12/2007

ability for cocrystals of pharmaceuticals relative to the crystalline free form of the active pharmaceutical ingredient (API).[5,12] Perusal of the literature shows that the behavior of formulated cocrystals has received little attention. This is certain to change as cocrystals move further into the development pipelines of pharmaceutical companies.

Celecoxib (4-[5-(4-methylphenyl)-3-(trifluoromethyl)-1*H*-pyrazol-1-yl]benzene-sulfonamide) is a well-studied inhibitor of the cyclooxygenase-2 enzyme (COX-2) and an anti-inflammatory drug, marketed under the trade name Celebrex.[19] The drug is reported to exist in four polymorphic modifications[20] with the stable form exhibiting poor water solubility (<1 μg/mL). However, the drug has been shown to be highly permeable using *in vitro* transport studies and has good absorption throughout the gastrointestinal tract (GI) as evidenced by the absorption profile in dog.[21] It has been demonstrated that both the rate and extent of drug absorption appear to be limited by dissolution rate of the marketed form. Since the drug is used for pain relief, many approaches to increasing the rate and extent of absorption have been tested and described in the literature. The approaches reported include the use of (1) higher energy polymorphs;[20,22] (2) amorphous composites;[23,24] (3) solutions in organic vehicles;[25,26] (4) salt forms in combination with precipitation/crystallization inhibitors;[27] and (5) nanoparticulate formulations.[28] Since the relationship between dissolution behavior and dog PK results has been studied for so many different approaches, celecoxib would seem to be an excellent model system for evaluating new form/formulation strategies.

Four polymorphs and several amide solvates of celecoxib have been previously described in the literature. Form III of celecoxib (**Cel-III**) is the marketed form of the drug and is the most stable and least soluble of polymorphs known at this time. Forms I and II (**Cel-I** and **Cel-II**) were first described in a patent application filed in 2000.[29] Pure **Cel-I** was prepared by evaporation of solvent from organic

(5) McNamara, D. P.; Childs, S. L.; Giordano, J.; Iarriccio, A.; Cassidy, J.; Shet, M. S.; Mannion, R.; O'Donnell, E.; Park, A. Use of a glutaric acid cocrystal to improve oral bioavailability of a low solubility API. *Pharm. Res.* **2006**, *23* (8), 1888−1897.

(6) Peterson, M. L.; Hickey, M. B.; Zaworotko, M. J.; Almarsson, O. Expanding the Scope of Crystal form Evaluation in Pharmaceutical Science. *J. Pharm. Pharm. Sci.* **2006**, *9* (3), 317−326.

(7) Remenar, J. F.; Morissette, S. L.; Peterson, M. L.; Moulton, B.; MacPhee, J. M.; Guzman, H. R.; Almarsson, O. Crystal engineering of novel cocrystals of a triazole drug with 1,4-dicarboxylic acids. *J. Am. Chem. Soc.* **2003**, *125* (28), 8456−8457.

(8) Rodriguez-Hornedo, N.; Nehm, S. J.; Seefeldt, K. F.; Pagan-Torres, Y.; Falkiewicz, C. J. Reaction Crystallization of Pharmaceutical Molecular Complexes. *Mol. Pharmaceutics* **2006**, *3* (3), 362−367.

(9) Trask, A. V.; van de Streek, J.; Motherwell, W. D. S.; Jones, W. Achieving Polymorphic and Stoichiometric Diversity in Cocrystal Formation: Importance of Solid-State Grinding, Powder X-ray Structure Determination, and Seeding. *Cryst. Growth Des.* **2005**, *5* (6), 2233−2241.

(10) Trask, A. V.; Motherwell, W. D. S.; Jones, W. Pharmaceutical Cocrystallization: Engineering a Remedy for Caffeine Hydration. *Cryst. Growth Des.* **2005**, *5* (3), 1013−1021.

(11) Trask, A. V.; Motherwell, W. D. S.; Jones, W. Physical stability enhancement of theophylline via cocrystallization. *Int. J. Pharm.* **2006**, *320* (1−2), 114−123.

(12) Variankaval, N.; Wenslow, R.; Murry, J.; Hartman, R.; Helmy, R.; Kwong, E.; Clas, S. D.; Dalton, C.; Santos, I. Preparation and Solid-State Characterization of Nonstoichiometric Cocrystals of a Phosphodiesterase-IV Inhibitor and L-Tartaric Acid. *Cryst. Growth Des.* **2006**, *6* (3), 690−700.

(13) Oswald, I. D. H.; Allan, D. R.; McGregor, P. A.; Motherwell, W. D. S.; Parsons, S.; Pulham, C. R. The formation of paracetamol (acetaminophen) adducts with hydrogen-bond acceptors. *Acta Crystallogr., Sect. B: Struct. Sci.* **2002**, *B58* (6), 1057−1066.

(14) Bettis, J. W.; Lach, J. L.; Hood, J. Effect of Complexation with Phenobarbital on the Biologic Availability of Theophylline from Three Table Formulations. *Am. J. Hosp. Pharm.* **1973**, *30* (240), 243.

(15) Higgins, W. M.; Dunker, M. F. W. Reaction of theophylline with barbiturates. *J. Am. Pharm. Assoc.* **1944**, *33*, 310−314.

(16) Nakao, S.; Fuji, S.; Tomita, K. The Crystal and Molecular Structure of the 2:1 Molecular Complex of Theophylline with Phenobarbital. *Acta Crystallogr.* **1977**, *B33*, 1373.

(17) McIntosh, J.; Robinson, R. H. M.; Selbie, F. R.; Reidy, J. P.; Elliot Blake, H.; Guttmann, L. *Lancet* **1945**, *249*, 97−99.

(18) Santesson, C. G. Addition combinations. *Arch. Exp. Pathol. Pharmakol.* **1926**, *118*, 313−324.

(19) *Physicians Desk Reference*, electronic library version, MicroMedex (Thomson Healthcare).

(20) Lu, G. W.; Hawley, M.; Smith, M.; Geiger, B. M.; Pfund, W. Characterization of a novel polymorphic form of celecoxib. *J. Pharm. Sci.* **2005**, *95* (2), 305−317.

(21) Paulson, S. K.; Vaughn, M. B.; Jessen, S. M.; Lawal, Y.; Gresk, C. J.; Yan, B.; Maziasz, T. J.; Cook, C. S.; Karim, A. Pharmacokinetics of celecoxib after oral administration in dogs and humans: effect of food and site of absorption. *J. Pharmacol. Exp. Ther.* **2001**, *297* (2), 638−645.

(22) Hawley, M.; Lu, G. W.; Geiger, B. M.; Smith, M. A.; Gao, P.; Hageman, M. J.; Ewing, G. D. Precipitation method for the preparation of a polymorphic crystalline form of the COX-2 inhibitor celecoxib. International Publication Number WO 2006/079923 A1, 2006.

(23) Gupta, P.; Chawla, G.; Bansal, A. K. Physical Stability and Solubility Advantage from Amorphous Celecoxib: The Role of Thermodynamic Quantities and Molecular Mobility. *Mol. Pharmaceutics* **2004**, *1* (6), 406−413.

(24) Hageman, M. J. Solid-state form of celecoxib having enhanced bioavailability. International Publication Number WO 2001/042221 A1, 2000.

(25) Hariharan, M.; Kararli, T.; Hassan, F.; Forbes, J. Rapid-onset formulation of a selective cyclooxygenase-2 inhibitors. International Publication Number WO 2001/078724 A1, 2001.

(26) Subramanian, N.; Ray, S.; Ghosal, S. K.; Bhadra, R.; Moulik, S. P. Formulation design of self-microemulsifying drug delivery systems for improved oral bioavailability of celecoxib. *Biol. Pharm. Bull.* **2004**, *27* (12), 1993−1999.

(27) Tawa, M.; Remenar, J.; Peterson, M.; Almarsson, Ö.; Guzman, H.; Chen, H.; Oliveira, M. Pharmaceutical compositions with improved dissolution. International Publication Number WO 2004/061433 A1, 2004.

(28) Shah, U.; Vemavarapu, C.; Galli, C. Preparation of pharmaceutical compositions containing nanoparticles. International Publication Number WO 2006/003504 A1, 2005.

(29) Ferro, L. J.; Miyake, P. J. Polymorphic crystalline forms of celecoxib. International Publication Number WO 01/42222 A1, 2000.

solutions, but it could also be prepared in lower purity by heating a dimethylacetamide (DMA) solvate to 100 °C for 48 h. Heating the DMA or DMF (*N*,*N*-dimethylformamide) solvate of celecoxib to 130 °C yielded a mixture of metastable form **Cel-II** and **Cel-III** by PXRD. The first demonstration of enhanced bioavailability or absorption rate from a polymorph other than **Cel-III** appeared in 2005 using newly described polymorph IV, **Cel-IV**.[20] The new form was prepared by adding a concentrated solution of celecoxib in PEG400/polysorbate 80 solution to solutions of HPMC and PVP in water, followed by addition of sweeteners and other additives suitable for an oral suspension. **Cel-IV** was isolated from the suspensions and shown to dissolve twice as fast, have 4-fold higher bioavailability than **Cel-III** powder, and be shelf-stable toward form conversion for periods of 16 months or longer at 25 °C.

The large number of different strategies tested to increase the rate and extent of celecoxib absorption in animal models, especially beagle dogs, make it an ideal drug for testing additional strategies and concepts. A recent review compared the absorption profiles of different formulation strategies in dogs and discussed the differences in terms of dissolution rates into 1% SDS and of the physical form and solubility of celecoxib when supersaturated in aqueous media.[30] Specifically, the extent of absorption of celecoxib from solutions in organic vehicles was lowest when the drug recrystallized as large aggregates within 5 min of dilution into water. These aggregates failed to dissolve in 1% SDS after 2 h unless sonicated, even though the drug started as a solution and there was enough SDS present to dissolve the full dose. Higher bioavailability was obtained from solutions of the drug in PEG 400, from which the drug precipitates out as a fine emulsion in water and slowly crystallizes over 15−20 min. Addition of crystallization inhibitors that prolonged supersaturation for over 30 min led to the highest and fastest absorption. Enhanced PK has also been demonstrated for amorphous composites of celecoxib with PVP[24] and suspensions of **Cel-IV**.[20] While the dissolution profiles for these formulations did not accompany the animal PK data, it is easy enough to prepare the formulations and study their dissolution properties in order to make the correlation. Another recently published study describes dissolution/supersaturation profiles associated with high bioavailability for seven different formulations of celecoxib salts or organic solutions with non-ionic surfactants as crystallization inhibitors.[27,31] The absolute proof of bioavailability enhancement still requires an animal study, but the overwhelming volume of data on celecoxib shows that it is possible to predict with reasonable confidence whether a formulation will increase absorption by considering both dissolution properties and form conversion in solution.

Scheme 1

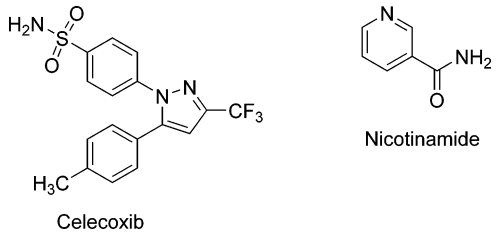

The discovery of a celecoxib:nicotinamide (**Cel:Nic**) cocrystal, shown in Scheme 1, presented an opportunity to showcase the importance of formulation strategies as part of evaluating the potential utility of a cocrystal. One could envision the possibility of polymorph formation upon removal of the amide cocrystal former by solubilization in water, analogous to polymorph formation upon evaporation of amide solvates. Likewise, a suspension of **Cel-IV** could result from dissolving the cocrystal in the presence of HPMC or PVP instead of starting with the concentrate of celecoxib in PEG/polysorbate that is currently used. The conversion of the cocrystal to celecoxib polymorphs in the presence and absence of PVP will be used to demonstrate the importance of formulation when evaluating the potential of a cocrystal to improve dissolution and bioavailability relative to the stable free crystalline form of a molecule.

The crystal structure of **Cel:Nic** will be presented along with physical characterization data and a description of the cocrystal's behavior in aqueous media. The studies include an assessment of the effects of small amounts of surfactants and PVP on conversion to polymorphs of celecoxib and/or amorphous material in acidic aqueous suspension in order to approximate the behavior of the compound when released into the stomach. It will be shown that the dissolution rate of the resulting suspensions into buffered 1% SDS is related to the physical form(s) present at the time this solubilizing medium is added.

Methods and Materials

Preparation of Cel:Nic. Procedure 1. Cel:Nic for the dissolution and characterization studies was crystallized by cooling a hot solution containing celecoxib (1.91 g, 5.01 mmol) and nicotinamide (0.644 g, 5.27 mmol) in chloroform (18 g) to room temperature. The slurry was allowed to stand for 10 min at room temperature and was then filtered by suction. The crystalline solid was rinsed with 3 mL of cold chloroform, initially dried on the filter paper for 10 min, and then transferred to a vacuum oven, where it was dried at 50 °C under house vacuum for 30 min. Dried aggregates were gently broken up with a mortar and pestle, and the solids were shaken periodically in an 850 μm sieve until all aggregates were small enough to pass through. The sieved solids were transferred to a clean vial and stored at room temperature without protection from ambient light.

Procedure 2. Cel:Nic was prepared by grinding celecoxib with 1.02 molar equiv of nicotinamide using a mortar and

(30) Remenar, J. F. Improving Oral Bioavailability through Inhibition of Crystallization after Dosing. *Am. Pharm. Rev.* **2007**, *10* (2), 84−89.

(31) Guzmán, H. R.; Tawa, M.; Zhang, Z.; Ratanabanangkoon, P.; Shaw, P.; Gardner, C. R.; Chen, H.; Moreau, J.-P.; Almarsson, Ö.; Remenar, J. F. Combined Use of Crystalline Salt Forms and Precipitation Inhibitors to Improve Oral Absorption of Celecoxib from Solid Oral Formulations. *J. Pharm. Sci.*, in press.

pestle, adding THF to form a thick paste, and then slowly evaporating the THF at 60 °C in a vial with a pinhole in the cap. Conversion was incomplete after a single cycle. Therefore, additional THF was added and subsequently evaporated to yield a powder where peaks of the starting materials were minimized.

Procedure 3. Crystals large enough for single crystal analysis were grown from chloroform spiked with dimethoxyethane (2.4% by volume). Five hundred milligrams of **Cel:Nic** prepared using procedure 1 above was dissolved in 2.5 mL of chloroform by heating and then filtered into a vial through a 0.2 μm nylon syringe filter. A 400 μL aliquot was pipetted into a clean vial, 10 μL of dimethoxyethane was added, and the sample was allowed to crystallize in an oven at 40 °C overnight. The sample was removed from the oven after 16 h, and the excess solvent was pipetted off of the crystals immediately.

Preparation of Cel-IV. Cel-IV was prepared and isolated using the procedure of Lu et al.[20] in order to obtain a reference spectrum and PXRD patterns for comparison to materials isolated from form-conversion studies with **Cel:Nic**.

Preparation and Characterization of 1/1 Celecoxib:PVP-K30 Amorphous Composite. A composite of 1/1 celecoxib:PVP-K30 was prepared according to the procedure of Gupta et al.[32] Microscopy, PXRD, and DSC were used to confirm that the sample was amorphous. The material was lightly ground for use in dissolution studies.

Physical Characterization. PXRD patterns were measured on a Bruker AXS D8 Discover X-ray diffractometer (Bruker-AXS, Madison, WI). The instrument was equipped with GADDS (general area diffraction detection system) software, a Bruker AXS HI-STAR area detector at a distance of 15.05 cm as per system calibration, a copper source (Cu Kα 1.5418 Å), automated *x-y-z* stage, and 0.5 mm collimator.

Thermal analyses were performed on a Q1000 mDSC and Q500 TGA (TA Instruments, Wilmington, DE). Heating rates of 10 °C/min were employed. The DSC was calibrated with a single-point method using the extrapolated onset of the melting point of a 0.275 mg sample of indium. Microscopy was performed using a Zeiss Axioplan microscope fitted with a Zeiss Axiocam type 1 SNO641 (Zeiss, Thornwood, NY).

Moisture sorption analysis was performed using a dynamic vapor sorption apparatus (Surface Measurement Systems, Monarch Beach, CA). Each sample was placed in a clean glass crucible and equilibrated in the apparatus at a specified relative humidity (RH) level. Varying the flow rates of dry nitrogen gas and saturated wet nitrogen gas streams controlled RH; the total combined flow rate was kept constant at 200 standard cubic meters per minute. After initial equilibration, RH was varied and change in mass was recorded over time as an indication of moisture sorption. A full humidity cycle is referred to as a ramp from 0% to 95% RH and back down to 0% RH. Mass equilibration at each humidity level was determined as a change in mass less than $\pm 2 \times 10^{-5}$ g over a time interval of 1 min (d*m*/d*t* of 0.002% min). After the assay, the change in mass was mathematically converted to water molar equivalents per dry compound molar equivalent.

NMR spectroscopy was performed using a Varian NMR system operating at 400 MHz with a 5 mm triple resonance probe. A sample of 20.2 mg of **Cel:Nic** was first dissolved in 1.0 mL of $CDCl_3$ and filtered prior to transferring to a 5 mm NMR tube. A ^{1}H NMR spectrum with 16 transients was measured. The aromatic protons of nicotinamide have relative areas varying from 0.99 to 1.09 while those of celecoxib vary from 1.09 to 1.28 per proton. The variability of about 10% for proton areas within the same molecule makes it difficult to quantitate the individual components, but it is clear that the stoichiometric ratio of components is 1:1 with a slight excess of celecoxib. It is not clear whether the excess is present within the cocrystal or as an external impurity, but it should be noted that crystalline celecoxib is not observed by PXRD or DSC.

Solid-state NMR spectroscopy was performed using a Varian NMR system operating at 400 MHz with a 4 mm HFX triple resonance MAS probe with the "X" nucleus tuned to carbon. ^{19}F CP/MAS spectra were collected with a spinning rate of 15 kHz, and temperature was controlled at 25 °C. ^{13}C CP/MAS spectra were measured spinning at 5 kHz using TOSS to suppress spinning side bands. A total of 64 scans were collected for each ^{19}F spectrum using a recycle delay of 10 s. The recycle delay was increased to 20 s for the pure **Cel-III** reference. A total of 512 scans were collected for ^{13}C spectra, using a recycle delay of 5 s since the two species of interest in the samples (PVP and **Cel-IV**) were both found to have T1 relaxation values on the order of 1−3 s. Vespel caps and spacers were used in the rotors to minimize ^{19}F background. PVDF was used as an external secondary reference using a chemical shift of −92 ppm for the central peak.

HPLC Methods. HPLC analysis was performed using a Waters Alliance 2690 HPLC equipped with a photodiode array detector and controlled by Empower software. Samples (10 μL) were injected onto a 4.6 × 30 mm Waters Symmetry C18 column with 3.5 μm particle size, maintained at 30 °C. The method was isocratic with a mobile phase of 0.1% TFA in 35/75 water/acetonitrile flowing at 1.0 mL/min. Data were collected for 6 min after injection at wavelengths from 200 to 400 nm, and the concentration was determined using peak areas extracted at 250 nm. A set of four standards from 0.024 to 0.30 mg/mL was used to calibrate the concentration/area curve daily.

Structure Determination from Powder Data. The structure determination was completed at an early stage of the project before conditions for crystalline **Cel:Nic** from solution were found. A sample was prepared according to procedure 2 above. A sample of **Cel:Nic** was lightly crushed and flame-sealed into a thin-walled glass capillary of 1.5 mm nominal diameter and mounted on the high-resolution

(32) Gupta, P.; Thilagavathi, R.; Chakraborti, A. K.; Bansal, A. K. Role of molecular interaction in stability of celecoxib-PVP amorphous systems. *Mol. Pharmaceutics* **2005**, *2* (5), 384−391.

Table 1. Crystallographic Parameters and Refinement Statistics

wavelength	0.69967(5) Å
lattice	$a = 46.483(3)$ Å
	$b = 9.9267(6)$ Å
	$c = 5.1930(3)$ Å
	$\beta = 94.106(1)°$
space group	$P2_1/a$
Rp: unweighted profile *R* factor	3.7%
Rwp: weighted profile *R* factor	4.22%
expected Rwp	1.45%
χ^2	8.48
coexisting nicotinamide	2% by weight
coexisting celecoxib	4.6% by weight
parameters refined	154
resolution: $\lambda/2\sin\theta$max	1.23 Å

powder diffractometer at beamline X3B1 of the National Synchrotron Light Source, Brookhaven National Laboratory. X-rays of wavelength 0.69967(5)Å were selected by a Si-(111) double crystal monochromator, and the radiation diffracted by the sample was analyzed by a Ge (111) crystal before a NaI scintillation detector. A monitor in the incident beam corrected for decay and fluctuations in the beam. Data were collected in steps of 0.005° from 2° to 33.175°, with counting time increasing quadratically from 2 to 18 s per point. The total data collection time was 16 h.

Small amounts of the two starting materials, celecoxib (CCDC Refcode DIBBUL)[33] and nicotinamide (NICOAM02 and NICOAM03)[34] were observed in the powder diffraction pattern. When peaks due to those two phases were removed, it was possible to index the powder pattern of the cocrystal. Accurate peak positions were extracted using TOPAS (Bruker v. 3),[35] and a monoclinic lattice of approximate dimensions $a = 52.25$ Å, $b = 9.925$ Å, $c = 5.19$ Å, $\beta = 117.48°$ was found with TOPAS figure of merit 16.51.[36] While this is a rather poor figure of merit, the correctness of the assignment is confirmed by the subsequent structure determination and refinement. It is also noted that a ratio on the order of 10:1 between longest and shortest lattice dimensions is an extremely challenging problem for powder indexing software. Analysis of unobserved peaks led to the hypothesis that the space group was $P2_1/a$. Lattice parameters were reduced and refined to the values shown in Table 1. Intensities of the cocrystal peaks were extracted by the Pawley method, in a calculation in which the two impurity phases were simultaneously modeled according to published structures.

The peak intensities and correlation matrix elements from the Pawley extraction were input to the program PSSP[37] in order to produce a candidate structure based on rigid bodies taken from the known structures of individual molecules. The best solution was loaded into TOPAS for further refinement. Initially, the only parameters refined were the location and orientation of each molecule, along with the torsions of major groups within the celecoxib. As the refinement progressed, it was possible to release restraints on much of the structure and still obtain a stable refinement with reasonable geometry. The best refinement that could be obtained without H atoms had a weighted *R* factor (Rwp) of 8.52%, but some of the bond lengths were outside of customary ranges. Adding H atoms, tethered to their C or N atoms, improved the fit considerably. The fluorine atoms of the celecoxib molecule in the cocrystal are clearly disordered; any refinement with a specific orientation for CF_3 is significantly worse than if it is modeled as two separate CF_3 groups, allowed to rotate independently, each with 50% occupancy. The powder refinement cannot reliably distinguish N from O, and so the assignment of atoms to the sulfonamide and amide groups cannot be made from the X-ray data alone. The rotation modulo 120° or 180° is well-defined, and atoms were assigned to favor N−H−O hydrogen bonded contacts. Likewise, the positions of H atoms are not reliable from the powder diffraction measurements. We have imposed planar geometry on the nicotinamide NH_2, and a pyramidal geometry, pointing away from the nearby oxygens on the sulfonamide group, has been imposed. In the final refinement, the background was modeled with a Chebyshev polynomial of 13th order, and lattice dimensions, size, strain, and thermal parameter of the two minority phases were refined. The (isotropic) thermal parameter of each non-C atom of the cocrystal was independently refined; values range from $B = 0.7$ to 8.0 Å^2 (u_{rms} from 0.1 Å to 0.3 Å). In view of the limited resolution of the powder diffraction measurement, these parameters are not true measures of thermal motion, but do indicate that there are no undetected errors in the structure as reported. Packing diagrams were prepared using Mercury (Mercury v. 1.4.1 copyright CCDC 2001−2005).

Single Crystal. Data were collected on a Bruker Kappa APEX-II diffractometer equipped with an Oxford Cobra Cryo-system. A fragment of a crystal was excised from a longer needle and mounted on the diffractometer using Paratone-N oil and a MiTeGeN micromount on a Crystal Cap copper magnetic mount. Data were collected using 5 min frames to ensure diffraction to about 0.9 Å. Evaluation of the diffraction spots during the data collection indicated

(33) Vasu Dev, R.; Rekha, K. S.; Vyas, K.; Mohanti, S. B.; Kumar, P. R.; Reddy, G. O. Celecoxib, a COX-II inhibitor. *Acta Crystallogr., Sect. C: Cryst. Struct. Commun.* **1999**, *C55* (12), IUC9900161.

(34) Miwa, Y.; Mizuno, T.; Tsuchida, K.; Taga, T.; Iwata, Y. Experimental charge density and electrostatic potential in nicotinamide. *Acta Crystallogr., Sect. B: Struct. Sci.* **1999**, *B55* (1), 78−84.

(35) Bruker AXS. *General profile and structure analysis software for powder diffraction data—Users Manual* [Computer Program]; Bruker AXS: Karlsruhe, Germany, 2005.

(36) Coelho, A. A. Indexing of powder diffraction patterns by iterative use of singular value decomposition. *J. Appl. Crystallogr.* **2003**, *36* (1), 86−95.

(37) Stephens, P. W.; Huq, A. PSSP: an open source powder structure solution program for direct space simulated annealing. *ACA Trans.* **2002**, *37* (Crystal Structure Determinations from Powder Diffraction Data), 125−142.

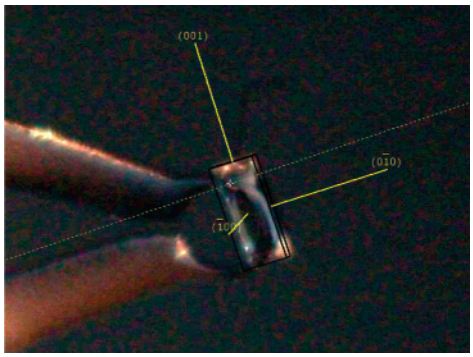

Figure 1. Photograph of the crystal used for the single-crystal data collection. The faces were indexed using a monoclinic unit cell of a = 46.1100(77) Å, b = 9.8843(21) Å, c = 5.0991(10) Å, β = 94.930(1)°.

that the crystal was twinned. After the data collection was complete Cell-Now was used to evaluate the unit cell and to attempt to understand apparent twinning. Cell-Now found a unit cell of a = 5.104 Å, b = 9.11 Å, c = 46.169 Å, α = 89.73°, β = 95.11°, γ = 90.33°. At least three domains were present. Data were integrated using Saint as implemented in the Bruker APEX suite of programs (v2.0.2). After integration and refinement the final monoclinic unit cell parameters were a = 5.0991(10) Å, b = 9.8843(21) Å, c = 46.1100(77) Å, β = 94.930(1)°. This cell was transformed using the matrix {(0 0 1)(0 −1 0)(1 0 0)] to bring it into the same setting as the powder structure resulting in a unit cell of a = 46.1100(77) Å, b = 9.8843(21) Å, c = 5.0991(10) Å, β = 94.930(1)°. The extent of the twinning and the weak intensity of the data prevented the satisfactory determination of a single-crystal structure. The similarity between the unit cells from the single-crystal data and that obtained by indexing the powder data gives added support to the structure solution from powder data. The crystal faces were indexed using the transformed unit cell from the single-crystal data, as shown in Figure 1. Face indexing shows that the short unit cell axis is aligned along the needle axis of the crystal and that the long unit cell axis is aligned along the shortest axis of the crystal.

Formulations for Dissolution Studies. The excipients used to prepare formulations included polyvinylpyrrolidone, PVP-K30 (Spectrum), and sodium dodecylsulfate, SDS (ICN Biomedicals, Inc.). Components were gently ground with **Cel:Nic** to ensure complete mixing. For the series of mixtures containing solid SDS, a blend of 400 mg of PVP-K30 and 100 mg of SDS was thoroughly ground together to distribute the SDS evenly on the PVP. This 4/1 PVP/SDS blend was used as is to prepare a formulation containing 11% SDS. The blend was further diluted with PVP and ground using the amounts shown in Table 2 to prepare the **Cel:Nic**/PVP mixtures containing 3.5% and 1% SDS.

***In Vitro* Dissolution of Cel:Nic, Method 1. Dissolution into 1% SDS.** Samples containing approximately 20 mg of celecoxib (as **Cel-III** or **Cel:Nic**) were transferred to a beaker with a magnetic stir bar, and 50 mL of 1% SDS in 20 mM sodium phosphate buffer at pH 6.5 and 37 °C was added.

Table 2. Excipients Added to 200 mg of **Cel:Nic** To Prepare Formulations

formulation	amounts of each component weighed to ±2 mg
1/1 **Cel:Nic**/PVP	200 mg of PVP-K30
11% SDS + 1/1 **Cel:Nic**/PVP	250 mg of 4/1 PVP-K30/SDS
3.5% SDS + 1/1 **Cel:Nic**/PVP	75 mg of 4/1 PVP-K30/SDS + 140 mg of PVP-K30
1% SDS + 1/1 **Cel:Nic**/PVP	25 mg of 4/1 PVP-K30/SDS + 180 mg of PVP-K30

At selected time points, 1.0 mL aliquots of the solution/suspension were filtered using a 0.2 μm nylon syringe filter. The first 0.3 mL of filtrate was discarded, and 0.4 mL aliquots were immediately transferred to a HPLC vial and diluted with 0.4 mL of acetonitrile. The samples were crimp sealed and assayed within 6 h of preparation by HPLC. After the final time point, the samples were sonicated briefly to dissolve any remaining aggregates. An aliquot of each sonicated solution was taken, filtered, diluted, and assayed as described above to establish the concentration of "100% dissolved" after accounting for solids lost during filtration.

***In Vitro* Dissolution of Cel:Nic, Method 2. Suspension To Allow for Form Conversion Prior to Dissolution into 1% SDS.** Weighed solids containing the equivalent of 20 mg of celecoxib were placed in a beaker and suspended in 10 mL of 0.01 N HCl at 37 °C with or without 0.05% SDS or Triton-X100 to aid in wetting for a target concentration of 2 mg/mL. The equilibrium solubility of celecoxib in these media was determined to be <0.03 mg/mL. After 5 min, aliquots were removed to collect solids. The aliquots were transferred into the filter baskets of centrifuge filter tubes with 0.2 μm nylon membranes. The samples were centrifuged for 1 min, and the solids were analyzed immediately by PXRD to determine the form of solid present. After 15 min, 40 mL of 1.25% SDS in 25 mM sodium phosphate buffer at pH 6.8 was added to yield a final target concentration of 0.4 mg/mL celecoxib, 1% SDS, and 20 mM phosphate. Aliquots were taken at 5, 10, 20, 30, 45, and 60 min and then filtered, diluted, and assayed by HPLC as described in the previous paragraph.

***In Vitro* Dissolution of Cel:Nic, Method 3. Test for Supersaturation and Form Conversion.** Weighed solids containing the equivalent of 20 mg of celecoxib were placed in a beaker and suspended in 10 mL of 0.01 N HCl at 37 °C with or without 0.05% SDS or Triton-X100 to aid in wetting for a target concentration of 2 mg/mL. Samples were taken at 15, 30, 45, and 60 min and prepared as above for PXRD analysis. If conversion to **Cel-III** was incomplete at 60 min, samples were monitored for a maximum of 5 days.

Isolation of Solids from Suspension of 1/1 Cel:Nic/PVP + 3.5% SDS and Determination of PVP Content. 223 mg of 1/1 Cel:Nic/PVP + 3.5% SDS were suspended in 36 mL of 0.01 N HCl at 37 °C for 15 min. The suspension was transferred into 4 × 14 mL centrifuge tubes (12 mL per tube) and centrifuged for 5 min at 6000 rpm. The supernatant was poured off except for ~1 mL in each tube. The solids were reslurried into the supernatant and combined in a single tube.

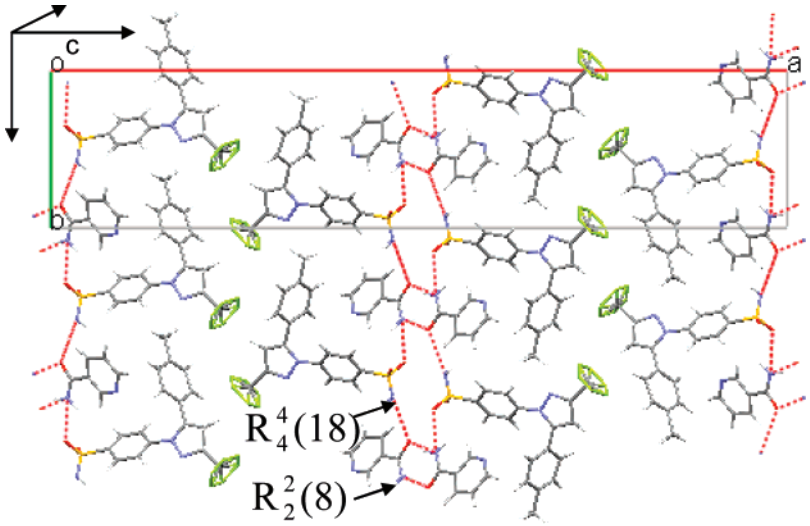

Figure 2. Packing diagram along the *ab* plane for **Cel:Nic** showing the hydrogen bonding motifs of and which propagate along the *b* axis. The structure is available from the Cambridge Crystallographic Data Centre as deposition number CCDC 639659, and is available via http://www.ccdc.cam.ac.uk/deposit.

After centrifuging a second time, all but 1 mL of the supernatant was poured off and the thick slurry was pipetted into the filter baskets of 2 × 1.0 mL microcentrifuge tubes with 0.35 μm filters. The samples were centrifuged for 3 min at 13000 rpm. Most of the liquid remained on top of the solids rather than filtering. The supernatants were again pipetted off, and the centrifuging continued for 5 min. The wet solids were transferred to a tared vial using a spatula and weighed. The initial mass was 244.1 mg. The solids were dried to constant weight under nitrogen with gentle heating. The final mass was 59.9 mg. TGA showed loss of 1.3% mass between room temperature and 150 °C. The amount of water in the solid was 244.1 − 59.9 mg = 184 mg of water. The concentration of PVP-K30 was 2.97 mg/mL assuming full dissolution. Therefore, the theoretical amount of PVP in the solids after evaporation of the water is 0.55 mg or <1% of the solids.

10.0 mg of the solids was dissolved in 1/1 acetonitrile/water and diluted for HPLC. The calculated mass of celecoxib in the sample (based on HPLC area) was 7.9 mg, or 7.9% of expected. The sample therefore contains approximately 20% of solid other than celecoxib. A repeat of the suspension/isolation experiment provided 27% solids other than API. FTIR and ^{13}C CP/MAS NMR spectroscopy showed a large component of PVP in the sample. The contribution from SDS was not determined.

Particle Size Measurement. Particle size was measured using a Zetasizer 3000 (Malvern Instruments, model DTS 5301) controlled by Malvern PCS software version 1.61. The CONTIN analysis method available in the Malvern PCS v1.61 software was used to determine the particle size with the default parameter set. A reference standard (Nanosphere 97 nm ± 3 nm standard, Duke Scientific Corporation) was also measured and yielded a measured particle size of 100 nm. Following particle size determination, an aliquot of each sample was dissolved by addition of acetonitrile and the concentration was measured using HPLC. Two samples for particle size measurement were taken from a suspension that was prepared by adding a mixture of 3.5% SDS + 1/1 **Cel:Nic**/PVP to 0.01 N HCl at 37 °C and stirring for 30 min. PXRD analysis of the isolated solids was consistent with **Cel-IV**. One sample was the filtrate from an aliquot of the suspension that had passed through a 0.45 μm filter (Nanosep MF GHP, lot no. A10645384). The other sample was the supernatant of a second aliquot of the suspension after centrifuging in a tube without the filter to separate out the solids. The supernatant had a faint haze while the filtrate was clear. The samples were prepared by centrifuging at 11,000 rpm for 3 min in a benchtop centrifuge (Eppendorf 5415D, by Brinkmann).

Results and Discussion

Structure Description. The crystal structure of **Cel:Nic** was deduced from powder data, and is further supported by unit cell parameters from single-crystal data as described in the Methods and Materials section. Examination of the packing diagram indicates that the cocrystal is made up of hydrogen bonded bilayers where the trifluoromethyl groups orient to form the hydrophobic layer, as shown in Figure 2. Analysis of the hydrogen bond patterns indicates that the structure is built up from a series of rings, including $R_2^2(8)$ nicotinamide dimers and larger $R_4^4(18)$ rings.[38−41] The larger rings are composed of S═O···H and C═O···H hydrogen

(38) Bernstein, J.; Davis, R. E.; Shimoni, L.; Chang, N. L. Patterns in hydrogen bonding: functionality and graph set analysis in crystals. *Angew. Chem., Int. Ed. Engl.* **1995**, *34* (15), 1555−1573.
(39) Etter, M. C.; MacDonald, J. C.; Bernstein, J. Graph-set analysis of hydrogen-bond patterns in organic crystals. *Acta Crystallogr., Sect. B: Struct. Sci.* **1990**, *B46* (2), 256−262.
(40) Etter, M. C.; Urbanczyk-Lipkowska, Z.; Zia-Ebrahimi, M.; Panunto, T. W. Hydrogen bond-directed cocrystallization and molecular recognition properties of diarylureas. *J. Am. Chem. Soc.* **1990**, *112* (23), 8415−8426.

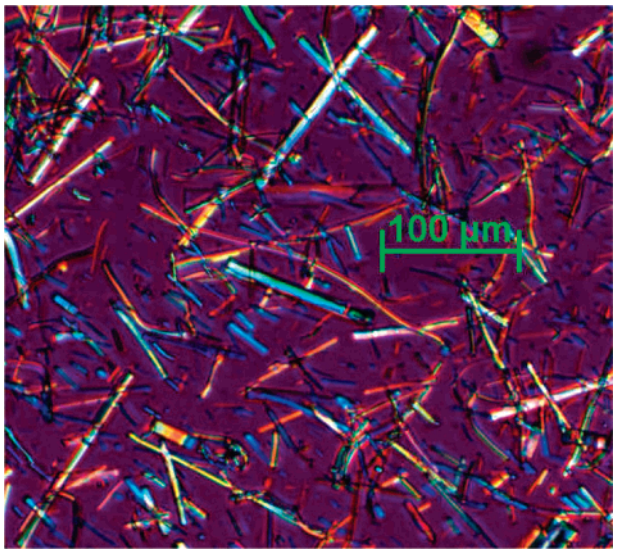

Figure 3. Photomicrograph of **Cel:Nic** needles shown at 10× magnification.

bonds from the sulfonamide group of the celecoxib molecules with the periphery of the nicotinamide dimers (Figure 2). Additional hydrogen bonding may be present within the $R_4^4(18)$ ring resulting in a $R_2^2(8)$ sulfonamide dimer and a $R_4^4(9)$ ring between nicotinamide and sulfonamide dimers. However, due to some ambiguity of the precise sulfonamide orientation this additional hydrogen bonding is speculative. There are also edge-to-face interactions between the aryl rings of the celecoxib molecules and the edge of the nicotinamide aryl ring. The hydrogen bonding interactions support double layers that expose the trifluoromethyl group and aryl edges on both sides to neighboring layers.

Characterization of Cel:Nic Crystals Grown from Solution. Cel:Nic can be prepared by crystallization of a hot chloroform solution containing celecoxib and nicotinamide in a 1/1.05 molar ratio. The resulting crystals appear as thin, birefringent needles under crossed polars as shown in Figure 3. The PXRD for the cocrystal is shown in Figure 4, along with patterns for the starting materials. The ratio of components was confirmed to be 1:1 by integration of the ^{1}H NMR spectrum of a dissolved sample of the cocrystal in $CDCl_3$, consistent with the crystal structure. The crystals have a sharp melting endotherm observed as a peak with maximum at 130 °C in the DSC. The material loses less than 0.25% weight on heating to 100 °C in the TGA. Finally, the compound is nonhygroscopic, undergoing less than 0.1% change in weight when cycled between 5% and 90% relative humidity at 25 °C. (Data for the full characterization and stability of the cocrystal are shown in the Supporting Information.) The cocrystal was found to be physically stable over a period of 4 weeks, both as a neat solid and in the formulations described in the following sections.

(41) Grell, J.; Bernstein, J.; Tinhofer, G. Graph-set analysis of hydrogen-bond patterns: some mathematical concepts. *Acta Crystallogr., Sect. B: Struct. Sci.* **1999**, *B55* (6), 1030−1040.

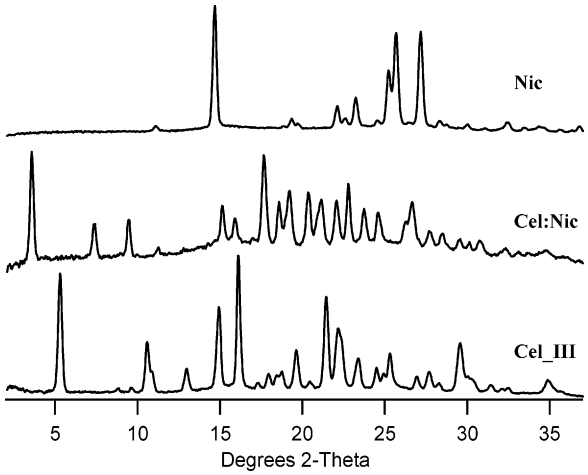

Figure 4. PXRD patterns of cocrystal constituents and **Cel:Nic** crystallized from chloroform.

Dissolution of Cel:Nic. Previous studies have shown that the rate and extent of celecoxib absorption increase when the rate of dissolution into 1% SDS is increased. Likewise, the absorption increases at higher concentrations of dissolved celecoxib. Absorption can be facilitated by dosing nanocrystalline **Cel-III**,[28] stabilized amorphous celecoxib, metastable polymorphs, and solutions in PEG400/water. However, dosing sodium salts or solutions of celecoxib from certain organic vehicles can result in lower overall bioavailability in animal models.[27,30] At first, these observations seem contradictory: if the rate of absorption is related to the rate of dissolution, then how could predissolved celecoxib in organic vehicles lead to reduced bioavailability? It has been suggested that rapid growth of large aggregates of **Cel-III** upon addition to aqueous media could be responsible for the lower bioavailability observed in such cases.[30] Properly assessing the dissolution of any new form of celecoxib should consider both the rate of dissolution relative to **Cel-III** into 1% SDS and characterization of the solids that form under supersaturated conditions.

Prior to initiating dissolution studies, the physical stability of **Cel:Nic** suspended in various aqueous media at 37 °C was studied to determine the potential for form conversion and growth of aggregates in biological fluids. Figure 5 shows the media tested and the PXRD patterns of solids isolated after 5 min in suspension. In the absence of SDS, samples in 0.01 N HCl converted to **Cel-I** within 5 min, but **Cel-III** grew in slowly over 30 min (full data set not shown). **Cel-I** is most easily distinguished from **Cel-III** by the presence of an isolated peak at 6.9° 2θ in the PXRD. The SDS-free sample in 20 mM phosphate at pH 6.5 was dominated by **Cel-III**, but there were traces of the metastable polymorph detectable at the 5 min time point. The ionic surfactant SDS was used to aid in wetting of the drug, since the exposed faces of the cocrystal are hydrophobic and are difficult to wet completely. All suspensions containing SDS completely converted to **Cel-III** within 5 min. Most surprising was the observation that a 5-fold dilution of the 0.01 N HCl + 0.9% NaCl solution led to a mixture of **Cel-III** and **CEL-II** while

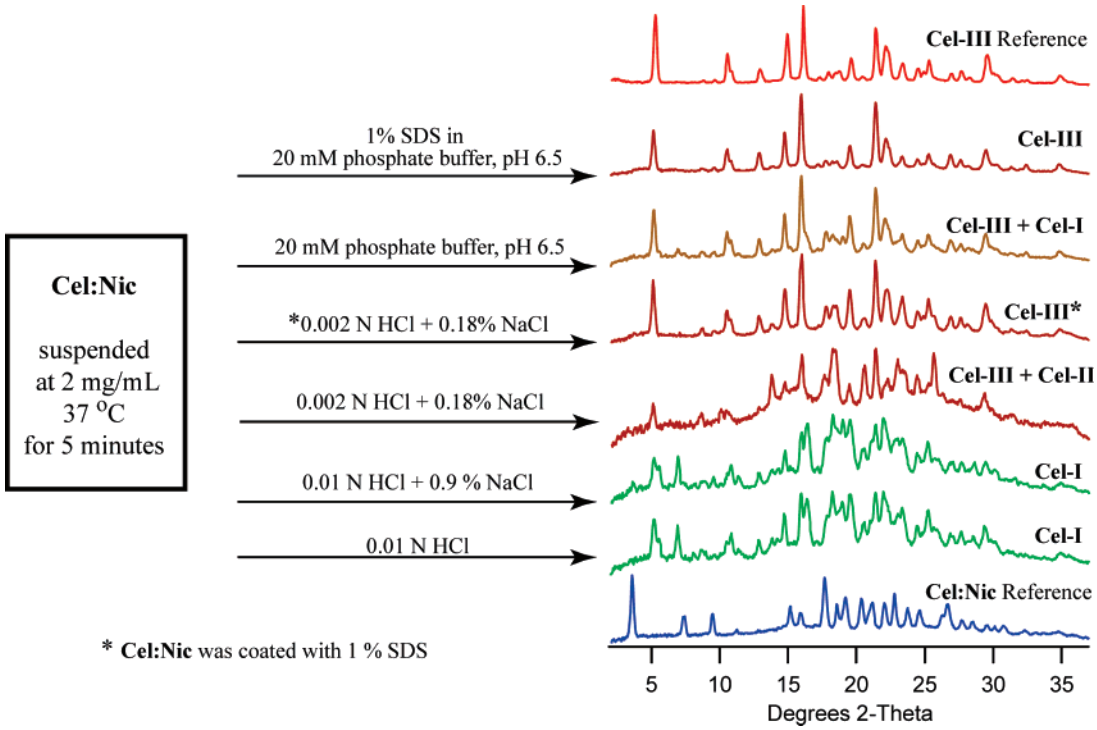

Figure 5. **Cel:Nic** form conversion after suspension for 5 min at 37 °C in aqueous media. * denotes that the Cel:Nic was coated with 1% SDS by gently grinding in a mortar and pestle prior to suspension in aqueous medium.

the undiluted medium provided **Cel-I**. **Cel-I** and **Cel-II** are known to be metastable relative to **Cel-III**, and they are typically only observed in time points between 5 and 30 min when they appear.[29] The diluted acid system was included to simulate dilution of stomach acid by drinking a glass of water, assuming a resting volume of 50 mL of gastric fluid and a 200 mL glass of water. From these results, it is clear that conversion of neat **Cel:Nic** to crystalline forms of celecoxib is rapid, and that evaluation of the cocrystal dissolution must take into account these physical form changes. It also indicates that the nicotinamide rapidly dissolves away from the cocrystal and remains in solution.

The effect of **Cel:Nic** conversion to **Cel-I** and **Cel-III** on the dissolution rate was tested using a target celecoxib concentration of 0.4 mg/mL in 1% SDS at pH 6.5, where celecoxib was found to have an equilibrium solubility of ~0.55 mg/mL. The experiment was intended to simulate release of **Cel:Nic** into a fasted stomach at pH 2, where absorption of drug is minimal and form conversion can occur, followed by transfer into the intestines where the pH is closer to 6.5 and material is absorbed as it dissolves. While there are significant variations in gastric contents and residence times between individuals on different days, this type of study should be able to indicate the potential for variability in dissolution rates when dosing the neat cocrystal.

Figure 6 compares the dissolution profiles for **Cel-III** and **Cel:Nic** added directly to 1% SDS with those of **Cel:Nic** after conversion to forms **Cel-I** and **Cel-III** in suspension. The concentration of dissolved celecoxib reaches approximately 80% of target within 5 min of adding **Cel:Nic** directly to a 1% SDS solution at a target celecoxib concentration of 0.4 mg/mL. In comparison, only about 50% of **Cel-III** dissolves in the first 5 min, and the dissolution does not reach 80% until the 30 min time point. Any solids remaining after 5 min in the **Cel:Nic** experiments dissolve more slowly, consistent with the conversion of undissolved material to **Cel-III**. Likewise, when presuspension in 0.01 N HCl for 15 min leads to conversion to metastable **Cel-I**, the initial profile of dissolution is intermediate between that of **Cel-Nic** and **Cel-III**. The PXRD patterns at 5 min confirm conversion of the cocrystal to **Cel-I**. However, longer interval studies have shown that the metastable form slowly converts to **Cel-III** over 30 min in suspension, with a mixture of the two forms clearly present at 15 min. In cases where there is significant conversion to **Cel-III** prior to diluting the suspension with the dissolution medium, the percentage of material dissolved at 5 min is lower than that for as received **Cel-III**, and a larger amount of solid remained after 60 min. This can be seen in the two dissolution curves where **Cel:Nic** was presuspended in 0.002 N HCl. In one of the two, neat **Cel:Nic** was presuspended with conversion to a mixture of **Cel-II** and **Cel-III**. In the other, **Cel:Nic** was gently ground with 1% solid SDS by weight prior to suspension, leading to a faster conversion to **CEL-III**. Further dissolution proceeds slowly over several hours unless the sample is sonicated briefly. Microscopic evaluation of solids remaining after 60 min revealed that **Cel-III** crystallizes as large aggregates of fine needles as shown in Figure 7. It cannot be determined from these studies whether **Cel-II** has an impact on the observed dissolution rate, but it should be noted that both of these suspensions contained large aggregates that failed

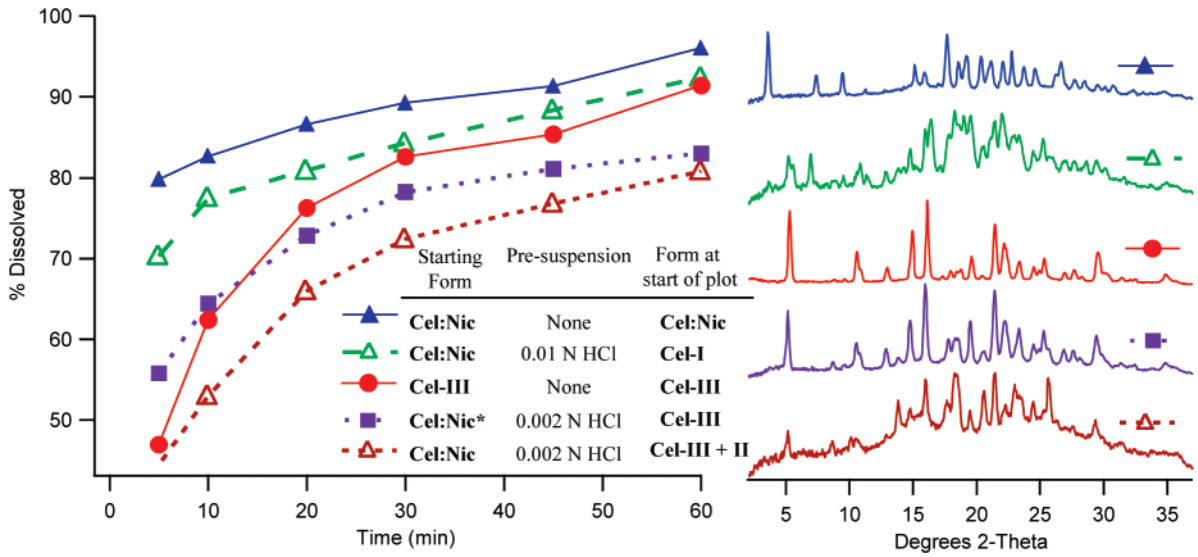

Figure 6. Dissolution into 1% SDS in pH 6.5 phosphate buffer at 37 °C with a target concentration of 0.4 mg/mL, and PXRD patterns of the solid phases at the approximate the time of SDS addition. For samples subjected to a "presuspension", **Cel:Nic** was suspended at 2 mg/mL in the listed medium for 15 min prior to 5-fold dilution with 1.25% SDS in 25 mM phosphate buffer at pH 6.8.

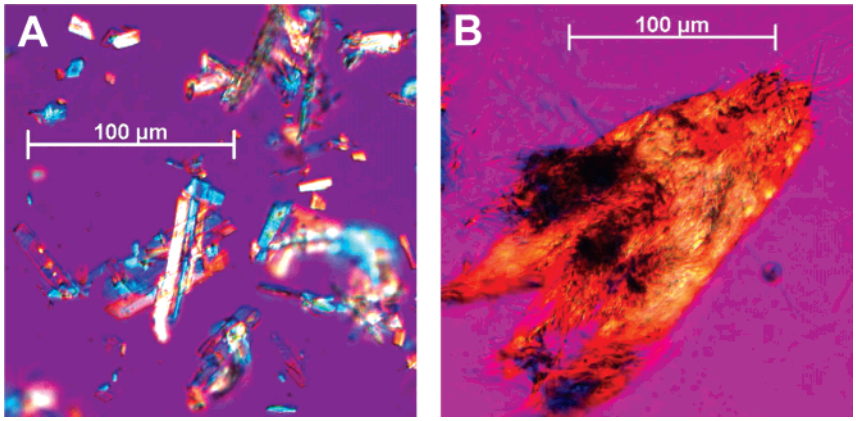

Figure 7. Comparison of (A) **Cel-III** as used in dissolution experiments and (B) slowly dissolving aggregates of **Cel-III** formed by suspending **Cel:Nic** in 0.01 N HCl with 0.05% added SDS at 37 °C and a target celecoxib concentration of 2 mg/mL.

to dissolve in the first 60 min after dilution into 1% SDS solution.

The combined data clearly indicate a dissolution rate advantage of **Cel:Nic** over **Cel-III**; however, celecoxib recrystallizes rapidly in aqueous media unless there is another phase for it to partition into (SDS in the case of a dissolution study). The polymorphic form and the size of the crystals/aggregates that form appear to be sensitive to relatively minor changes in the dissolution medium even, such as a 5-fold change in HCl concentration. When the medium is changed to one that has the capacity dissolve to the celecoxib, the observed dissolution profile varies to reflect the differences in the precipitated materials.

In attempts to rationalize the dissolution and form conversion behavior, the faces of a single crystal of **Cel**:**Nic** were indexed. The largest crystal faces, {001} and {010}, would likely expose aryl and trifluoromethyl functionality. The relatively hydrophobic nature of the aryl and trifluoromethyl functional groups at the crystal surfaces may explain the poor wetting characteristics of this material in the absence of surfactants. Surfactants that are able to promote wetting of **Cel:Nic** would allow the cocrystal to dissolve more rapidly. Due to the larger difference in the aqueous solubility of celecoxib and nicotinamide it is likely that the effective dissolution rates of the two species from the cocrystal are very different.

The crystal structure of **Cel-III**[33] has two molecules of drug hydrogen bonded to form a dimer with an $R_2^2(18)$ motif, as shown in Figure 8. These dimers stack into columns by C(4) chains through the sulfonamide groups with one sulfonamide oxygen atom left free of any hydrogen bonding interactions. These columns of dimers pack together by edge-to-face interactions along the *c*-direction of the crystal. With the exception of the exposed sulfonamide oxygen atom the columns of dimers expose hydrophobic trifluoromethyl and aryl functionalites. While even amorphous celecoxib is poorly

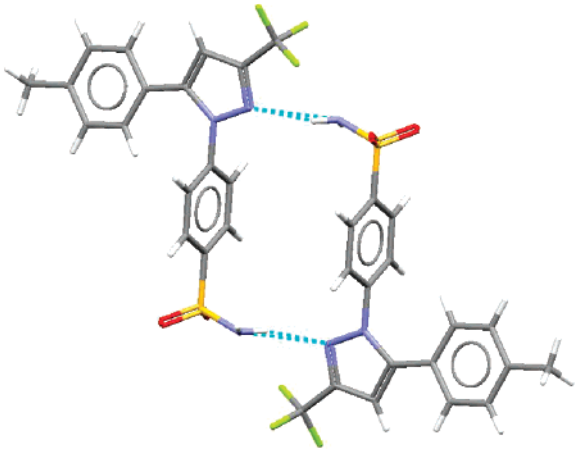

Figure 8. Dimer from the crystal packing of **Cel-III**.

soluble, one must consider that the hydrogen bonding arrangements and crystal packing contribute to the observed solubility of a given form.

The $R_2^2(18)$ dimer found in **Cel-III** is not preserved in the cocrystal. Formation of this dimer by collapse of the **Cel:Nic** lattice after removal of nicotinamide would require large scale molecular motion and reorganization of hydrogen bonding interactions. Collapsing the lattice of a cocrystal that lacks major motifs of **Cel-III** could lead to amorphous material, a metastable polymorph, or **Cel-III** itself. Once added to water, **Cel:Nic** could behave similarly to any other amorphous composite, a melt, a water-miscible organic solution, a salt with neutralizing agent, or any metastable crystalline form in water.

Performance Enhancement with PVP. Previously published animal studies have suggested a correlation between poor celecoxib absorption and the growth of celecoxib aggregates from salts or organic solutions.[29,30] Hence, studies were conducted to determine whether a commonly used pharmaceutical excipient, PVP, could prevent the rapid conversion of **Cel:Nic** to large aggregates of **Cel-III**. Several studies have shown that celecoxib can interact strongly with the widely used pharmaceutical excipient PVP.[24,32,42] Plasma concentrations of celecoxib in dogs were shown to be twice as high for tablets incorporating solid composites of amorphous celecoxib and PVP relative to **Cel-III** in a capsule.[24] Since PVP can be used to stabilize amorphous celecoxib and bring about increased bioavailability relative to crystalline **Cel-III**, it was reasoned that PVP might be able to inhibit conversion of the cocrystal to the less soluble form.

A 1/1 mixture of **Cel:Nic** with PVP-K30 was prepared, and the fate of the cocrystal suspended in 0.01 N HCl, with and without added surfactants, was monitored by PXRD. Figure 9 shows PXRD patterns for solids recovered from suspension after 60 min. In the absence of any surfactant, the formulation is slow to wet and floats on the surface of the liquid, as is observed for the neat cocrystal. Isolation of

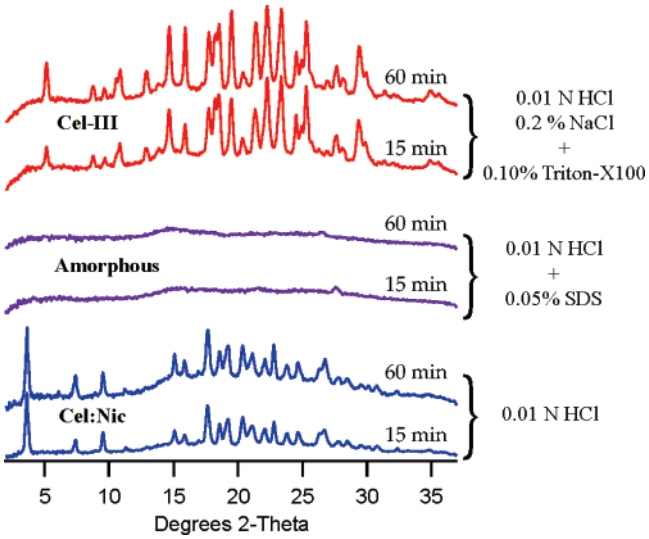

Figure 9. PXRD patterns of solids isolated from suspensions of 1/1 mixtures of **Cel:Nic** with PVP. The target concentration for all slurries was 2.0 mg/mL, and the temperature was maintained at 37 ± 2 °C.

the materials from the suspension suggests that the excipient might protect the cocrystal for up to an hour in the absence of a surfactant. However, considering the poor wettability of the mixture, it is likely that the sample includes some **Cel:Nic** that was shielded from contact with water. An effort was made to include suspended wet particles rather than only solids from the top, and the outer layer of floating aggregates was wet. Yet four samples taken over 60 min showed only the cocrystal. Closer examination of the PXRD patterns show a growing amorphous component superimposed on the **Cel:Nic** pattern. PVP-K30 alone wets and dissolves rapidly in the absence of celecoxib.

The effects of including low concentration surfactants in the suspension medium on wetting and form conversion were also investigated. Addition of SDS to the dissolution medium at a low concentration of 0.05% promotes rapid wetting of the mixture, and the cocrystal is lost within 5 min. However, the isolated solids appear to be predominantly amorphous by PXRD (Figure 9), rather than the aggregates of **Cel-III** that formed with the neat cocrystal. Using the non-ionic surfactant Triton-X100 also promoted rapid wetting, but **Cel-III** was isolated from the slurries. Addition of Triton-X100 at the same levels to suspensions of metastable forms of celecoxib was later shown to cause conversion to **Cel-III** while the suspensions remain stable for days with 0.05% SDS.

The results from the form conversion studies using the 1/1 mixture of **Cel:Nic** with PVP suggest that low concentrations of SDS can facilitate wetting of the formulation without promoting conversion to **Cel-III**. The formation of amorphous material in suspension with aqueous SDS is particularly enticing considering published reports of increased *in vivo* absorption of celecoxib from amorphous celecoxib/PVP composites relative to **Cel-III**. While not naturally present in the stomach, SDS is a solid surfactant

(42) Gupta, P.; Bansal, A. K. Molecular interactions in celecoxib-PVP-meglumine amorphous system. *J. Pharm. Pharmacol.* **2005**, *57* (3), 303−310.

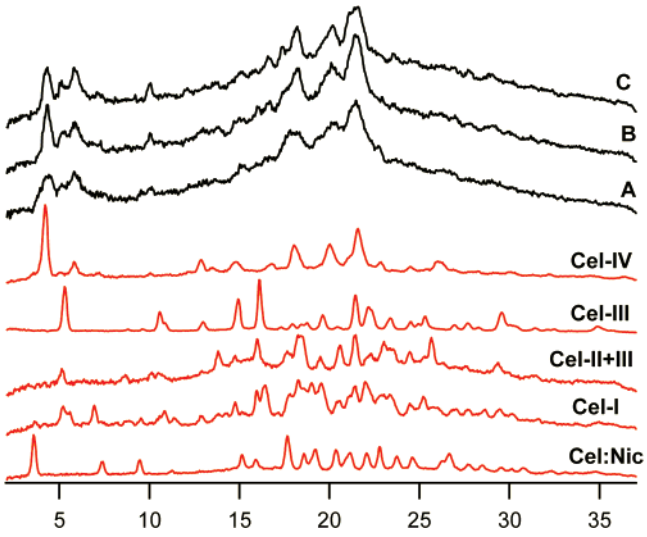

Figure 10. PXRD of solids collected from suspensions of mixtures containing 1/1 **Cel:Nic**/PVP-K30 with added SDS after 15 min at 37 °C. The SDS loading is (A) 1.2%, (B) 3.5%, (C) 11.1% by total weight of solids. Reference spectra are included for comparison.

that is present in many marketed drug products. Therefore, SDS was added to the **Cel:Nic**/PVP blend at up to 11% loading, which corresponds to incorporation of 50 mg of SDS per 200 mg of celecoxib, the amount of drug in the largest commercial capsule of celecoxib.[43] Additional loadings included 3.5% and 1.2% SDS by total weight of solids in the blends. These mixtures all wet within 5 min of addition to 0.01 N HCl, and the PXRD patterns were very broad, consistent with a large amorphous component as shown in Figure 10. However, the PXRD patterns also show new, broad peaks at 4.3°, 5.8°, 18.4°, 20.1°, and 21.5° 2θ that are inconsistent with the cocrystal or polymorphs I−III of celecoxib.

The suspension resulting from the mixture with 3.5% SDS was characterized more extensively. The new PXRD pattern consists of peaks that are considered to be characteristic of **Cel-IV**, recently disclosed in the literature, but the peaks are very broad, which could be due to a large disordered or amorphous component or a very small particle size.[20,22] The PXRD peak at 4.2° 2θ is uniquely low among celecoxib polymorphs and is present in the isolated solids. Another distinguishing feature of **Cel-IV** is the group of three peaks between 18° and 21.5° 2θ. One anomaly is the relatively large size of the peak at 5.8° 2θ, but the angle does coincide with a known peak that is a characteristic peak of **Cel-IV**. The available reference spectrum for **Cel-II** is of poor quality and mixed with **Cel-III**, but the pattern in the literature contains no peaks below 8° 2θ.

(43) The FDA's list of inactive ingredients shows oral tablets containing as much as 50 mg of SDS as found in an "Inactive Ingredient Search" for Approved Drug Products, Search for "SODIUM LAURYL SULFATE" U.S. Food and Drug Administration, Center for Drug Evaluation and Research. http://www.accessdata.fda.gov/scripts/cder/iig/index.cfm.

The composition of the suspended solids was further evaluated by performing the form conversion on a larger scale and isolating and characterizing the resulting solids. The solids were collected from suspension of both the 1% and 3.5% SDS blends and then dried to contain less than 1.3% volatiles between room temperature and 150 °C by TGA. The FTIR spectrum in Figure 11B shows a peak at 1598.7 cm^{-1} which is common to **Cel-IV** prepared in the literature and shifted from the value of 1594.9 cm^{-1} in **Cel-III**. An additional distinct peak common to **Cel-IV** and the isolated material is present at 3293.9 cm^{-1}. ^{19}F CP/MAS NMR spectroscopy also supports the assignment of the crystalline material as **Cel-IV** showing a pair of peaks for both the reference standard and the solids from suspension, while only a single ^{19}F peak is observed for **Cel-III**, as shown in Figure 12. However, while both **Cel-IV** peaks are present in the spectrum of the solids isolated from suspension, there is a broadening that is consistent with an amorphous component. The DSC trace for the dried solids showed a broad endothermic transition with four minima between 116 and 142 °C, the highest of which is 8 °C lower than the melting transition reported for **Cel-IV**. The lower value may be a depression related to PVP content or amorphous celecoxib.

The presence of 21−27% PVP in the solids isolated from suspension of the **Cel:Nic**/PVP/SDS blend was confirmed using a combination of FTIR, ^{13}C CP/MAS NMR spectroscopy, and HPLC showing that the solids obtained from two separate experiments contain only 78% and 72% celecoxib by weight. This represents an increase of greater than 30-fold in PVP concentration relative to what would be expected if the PVP was fully dissolved in the water. Since PVP is water soluble without the API and the centrifugation step leaves nanocrystalline celecoxib in suspension (see below) at up to 0.7 mg/mL, it stands to reason that PVP must have some increased affinity for part of the suspended celecoxib, possibly as a composite with the amorphous material. The same results are obtained when the mixture only contains 1% SDS, and also when the solids are collected by the alternative procedure of forcing the supernatant through an 0.2 μm filter and rinsing with 0.5 mL of water instead of by centrifugation.

Aliquots of the bulk suspension viewed under the microscope were found to have very small particles (<1 μm) that were observed visually, but that were difficult to photograph accurately due to the high magnification required to see them and the continuous motion of particles in suspension. Photomicrographs obtained for small clumps that settled to the bottom of the suspension and for solids collected on a centrifuge filter are shown in Figure 13, A and B, respectively. The small clumps appear to be transparent and amorphous, but are peppered with birefringent specs. Likewise, solids collected by filtration appear to be a mixture of transparent and birefringent components. Overall, the materials appear to be largely amorphous by microscopy, with micron-sized or smaller crystals trapped inside. This observation is somewhat different than the spectroscopic data would

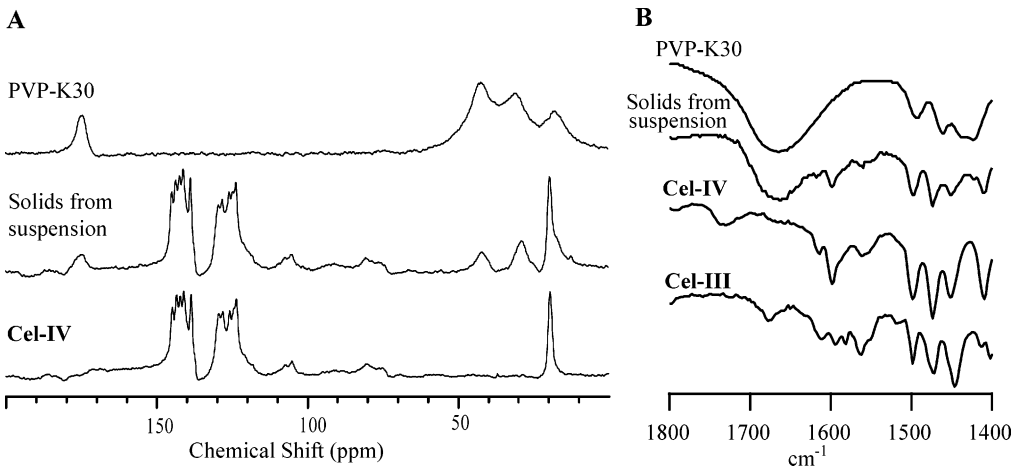

Figure 11. Spectra of solids isolated after suspending a blend of 1/1 **Cel:Nic**/PVP + 3.5% SDS in 0.01 N HCl for 15 min. The (A) ^{13}C CP/MAS and (B) FTIR data are both consistent with the presence of a large component of PVP. HPLC analysis of the solids suggests approximately 21% PVP by weight in the solids.

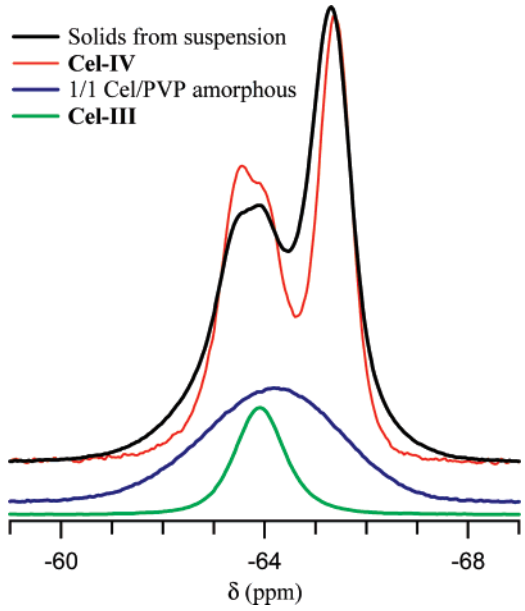

Figure 12. ^{19}F CP/MAS NMR spectra of reference samples and of freshly isolated solids isolated from a suspension a 1/1 **Cel:Nic**/PVP + 1% SDS by weight in 0.01 N HCl at 37 °C for 15 min.

suggest, where there is evidence for amorphous material, but it does not appear to be more than 10−20% of the total. It is possible that there was a larger amorphous component in suspension and that it crystallized as **Cel-IV** while drying in the presence of seed crystals, but quantitating the crystalline vs amorphous content by microscopy with such small particles is not possible.

The solubility of celecoxib in the suspension resulting from the mixtures of 1.1−11% solid SDS with 1/1 **Cel:Nic**/PVP was evaluated. In theory, the measured solubility should be similar to that of **Cel-III** with a similar amount of SDS and PVP. Otherwise, there would be a strong driving force for **Cel-III** to crystallize from the suspension and it would not remain stable for several days as observed. As expected, HPLC analysis of filtrates from centrifuge filtration found celecoxib concentrations to be undetectable at the low surfactant concentration, less than 1 μg/mL for 3.5% SDS, and only 5 μg/mL with 11% SDS. However, the corresponding supernatants were found to contain significant concentrations of celecoxib ranging from 0.1 to 0.7 mg/mL, despite having only a barely perceptible haze. Analysis of the hazy supernatant using DLS found an average particle size of 380 nm. Therefore, while the actual solubility of the sample is vanishingly low, it appears that a large portion of the crystalline material is present as a nanosuspension. Since the target concentration of celecoxib in these suspensions was approximately 2 mg/mL, it appears that 10−30% of the celecoxib remains suspended as ~380 nm particles after the chosen centrifugation conditions.

The dissolution rate of the suspension obtained from the mixture of 1/1 **Cel:Nic**/PVP + 1% SDS was measured to assess enhancement relative to **Cel-III** and unformulated **Cel:Nic**. Figure 14 compares the dissolution profiles obtained after adding buffered SDS to slurries in 0.01 N HCl from **Cel-III**, **Cel:Nic**, their blends with 2% SDS on PVP, and a 1/1 amorphous composite of celecoxib/PVP. More than 90% of the total drug dissolves within 1 min of diluting the slurry from 1/1 **Cel:Nic**/(2% SDS on PVP) into the SDS. The amorphous composite is slower in the first 2 min, but exceeds 90% dissolution after only 5 min. Both of these starting materials lead to optically clear solutions in SDS by 30 min. In contrast, **Cel-III** formulated with 2% SDS on PVP reaches only ~80% dissolution after 20 min, and still has visible solids at the 30 min time point. Importantly, the residual solids at the end of the **Cel-III** experiment do dissolve to yield clear solutions with sonication or continued stirring overnight. The same results were obtained when the final target concentration was reduced from 0.4 mg/mL to 0.32 mg/mL, thereby confirming that the effects were not overly sensitive to the degree of saturation. The blended **Cel:Nic** and **Cel-III** both provide enhanced dissolution rates compared to suspensions from the neat solids.

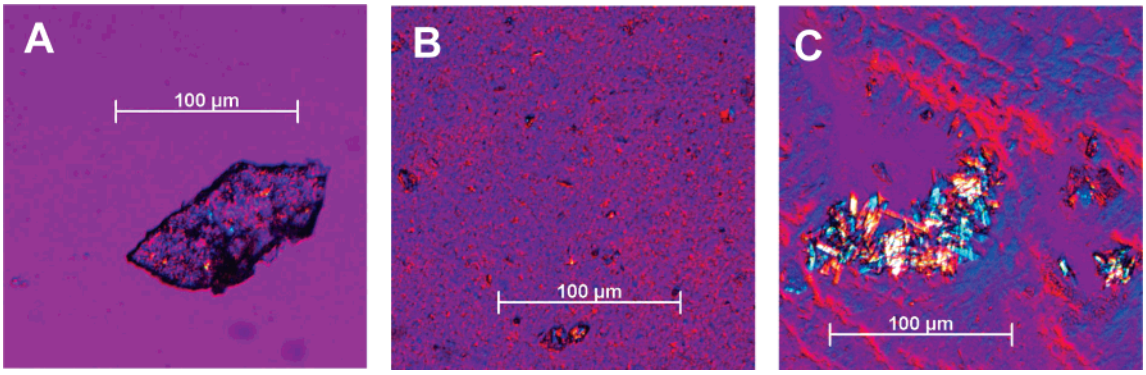

Figure 13. Microscope photos of solids isolated from a suspension of 3.5% SDS + 1/1 **Cel:Nic**/PVP at 37 °C in 0.01 N HCl: (A) a solid that settled out of a suspension, (B) solids collected by centrifuge filtration after 30 min in suspension, and (C) solids collected by filtration 14 h after adding 0.01% Triton-X100 to the suspension.

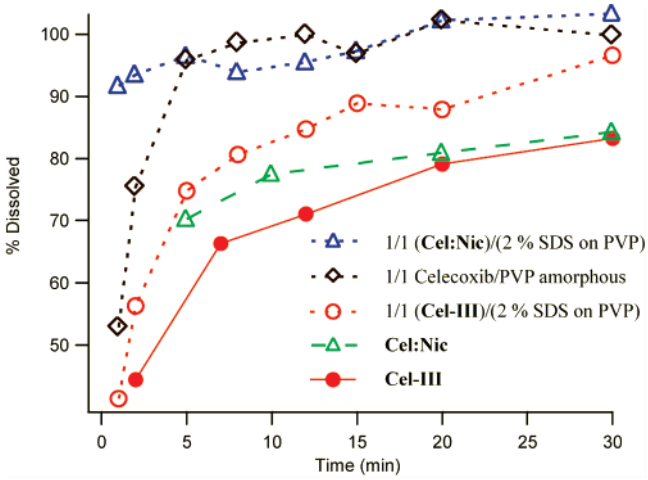

Figure 14. Dissolution into 1% SDS in pH 6.5 phosphate buffer at 37 °C with a target concentration of 0.4 mg/mL following a 15 min "presuspension", at a target concentration of 2 mg/mL in 0.01 N HCl at 37 °C. The ratio of celecoxib/PVP was identical for both **Cel-III** and **Cel:Nic**, with 1/1 ratio referring to wt/wt of **Cel:Nic**/PVP.

The suspension resulting from addition of the **Cel:Nic** blend with PVP and SDS is clearly primed to dissolve rapidly when introduced to an environment where equilibrium solubility has not yet been reached. The dissolution rate appears to be faster than that of amorphous composites of celecoxib that have previously been shown to be more completely absorbed in dog studies. Additionally, the crystalline material is present as **Cel-IV**, which is known to provide a >4-fold increase in maximum plasma concentration and total exposure in beagle dogs compared to neat **Cel-III**.[20] Last, **Cel-IV** crystallizes in this suspension as small particles, appearing as specs under the microscope and with many being on the order of 380 μm. It is well-known that such nanosized particles lead to higher bioavailability for a large number of poorly water-soluble pharmaceutical compounds.

The suspensions appear to be stable for days when solids are collected and examined by PXRD and microscopy. Indeed, seeding them with **Cel-III** does not seem to promote loss of **Cel-IV** and amorphous material over several days. However, the suspensions are in fact metastable as evidenced by conversion to **Cel-III** upon addition of the non-ionic surfactant Triton-X100. Clusters of **Cel-III** were visible among the amorphous material filtered from a suspension 18 h after adding of 0.01% Triton-X100. The crystallization proceeded faster at higher concentrations of Triton-X100 such that the growth of needles and clusters could be monitored under a microscope. Interestingly, the new crystals appear to grow from solution, suggesting that the amorphous material and **Cel-IV** dissolve prior to recrystallization. Low solubility and the choice of surfactant may both be important factors in the stability of the suspensions toward conversion to **Cel-III**.

Conclusions

The common practice of dosing poorly water soluble compounds as neat suspensions may not be ideal for materials that undergo dynamic dissociation processes in aqueous media. Uncontrolled conversion of dissociating forms after dosing into the gastrointestinal tract presents a potential complication demanding intervention. The rapid and uncontrolled form conversion of **Cel:Nic** in the absence of excipients could result in bioavailability that is inferior to that of **Cel-III** and lead to abandonment of a potential opportunity for improvement. The example presented here of the pharmaceutical cocrystal **Cel:Nic** illustrates the requirement to develop enhanced compositions using excipients, which can affect dissolution processes positively. Opportunities with excipient selection include stabilizing a cocrystal with good dissolution properties in suspension, or directing its conversion to intermediates that are associated with good oral absorption. The latter case is in evidence for **Cel:Nic**. We conclude that careful selection of crystal form of a low solubility compound, coupled with critical analysis of dissolution conditions and the dynamics of form conversion during contact with various simulated GI fluids, is an essential part of driving success in the complex process of pharmaceutical form selection.

The mixtures of SDS with 1/1 **Cel:Nic**/PVP are transformed to a suspension with the following characteristics

upon addition to 0.01 N HCl: (1) a portion of the drug becomes amorphous, presumably stabilized by PVP; (2) the crystalline material is present as a metastable polymorph, **Cel-IV**; and (3) the crystalline material present is mostly non-aggregated and has a very small particle size. All of the above characteristics have been shown to individually improve the absorption of celecoxib and/or other drugs in the literature. In this case the amorphous material, formation of metastable **Cel-IV**, and small particle size occur spontaneously on wetting a mixture of cocrystal with common excipients that appears to be shelf-stable. While this mixture has not been dosed to animals, the suspension formed after wetting does dissolve rapidly upon introduction of diluent that is commonly used to assess celecoxib dissolution, notwithstanding that there is a demonstrated benefit of faster dissolution rate for absorption of celecoxib published already in the literature.

This study of **Cel:Nic** highlights the importance of exploring formulation concepts for cocrystals in addition to studies of their structure, preparation, and scale-up. While rapid dissociation of **Cel:Nic** on wetting is an inherent property of the form, simple excipients can indeed capture the benefit of the cocrystal by trapping celecoxib as a mixture of rapidly dissolving species. The formation of incipient amorphous material, metastable polymorphs, and submicron particles upon oral dosing offers the possibility to achieve overall improvements in bioavailability from crystalline forms that are physically and chemically more stable on the shelf than the intermediate rapidly dissolving species themselves.

Acknowledgment. Use of the National Synchrotron Light Source, Brookhaven National Laboratory, was supported by the U.S. Department of Energy, Office of Science, Office of Basic Energy Sciences, under Contract No. DE-AC02-98CH10886. P.W.S. received financial support from TransForm Pharmaceuticals Inc. The TransForm authors wish to thank Dr. Örn Almarsson for insightful discussions regarding the relevance of the work to form selection, and for providing encouragement and time to develop concepts that are tangential to our primary responsibilities.

Supporting Information Available: Full characterization of the **Cel:Nic**, including the .cif file. This material is available free of charge via the Internet at http://pubs.acs.org.

MP0700108